

Modified climate with long term memory in tree ring proxies

This content has been downloaded from IOPscience. Please scroll down to see the full text.

2015 Environ. Res. Lett. 10 084020

(<http://iopscience.iop.org/1748-9326/10/8/084020>)

View the [table of contents for this issue](#), or go to the [journal homepage](#) for more

Download details:

IP Address: 193.134.202.245

This content was downloaded on 20/08/2015 at 11:21

Please note that [terms and conditions apply](#).

Environmental Research Letters

**OPEN ACCESS****RECEIVED**
25 March 2015**REVISED**
7 July 2015**ACCEPTED FOR PUBLICATION**
20 July 2015**PUBLISHED**
18 August 2015

Content from this work
may be used under the
terms of the [Creative
Commons Attribution 3.0
licence](#).

Any further distribution of
this work must maintain
attribution to the
author(s) and the title of
the work, journal citation
and DOI.

**LETTER**

Modified climate with long term memory in tree ring proxies

Huan Zhang¹, Naiming Yuan¹, Jan Esper², Johannes P Werner³, Elena Xoplaki¹, Ulf Büntgen^{4,5,6}, Kerstin Treydte⁴ and Jürg Luterbacher¹

¹ Department of Geography, Climatology, Climate Dynamics and Climate Change, Justus-Liebig University Giessen, D-35390, Giessen, Germany

² Department of Geography, Johannes Gutenberg University, Mainz, Germany

³ Department of Earth Science and Bjerknes Center for Climate Research, University of Bergen, Norway

⁴ Swiss Federal Research Institute WSL, Birmensdorf, Switzerland

⁵ Oeschger Centre for Climate Change Research, Bern, Switzerland

⁶ Global Change Research Centre AS CR, Brno, Czech Republic

E-mail: huan.zhang@geogr.uni-giessen.de

Keywords: climate reconstructions, tree-ring width, maximum latewood density, frequency domains

Abstract

Long term memory (LTM) scaling behavior in worldwide tree-ring proxies and subsequent climate reconstructions is analyzed for and compared with the memory structure inherent to instrumental temperature and precipitation data. Detrended fluctuation analysis is employed to detect LTM, and its scaling exponent α is used to evaluate LTM. The results show that temperature and precipitation reconstructions based on ring width measurements (mean $\alpha = 0.8$) contain more memory than records based on maximum latewood density (mean $\alpha = 0.7$). Both exceed the memory inherent to regional instrumental data ($\alpha = 0.6$ for temperature, $\alpha = 0.5$ for precipitation) in the time scales ranging from 1 year up to 50 years. We compare memory-free ($\alpha = 0.5$) pseudo-instrumental precipitation data with pseudo-reconstructed precipitation data with LTM ($\alpha > 0.5$), and demonstrate the biasing influences of LTM on climate reconstructions. We call for attention to statistical analysis with regard to the variability of proxy-based chronologies or reconstructions, particularly with respect to the contained (i) trends, (ii) past warm/cold period and wet/dry periods; and (iii) extreme events.

1. Introduction

Natural time series sometimes have a certain self-dependent structure, i.e. when an observation in a time series influences the following observations over a long period of time, this behavior is known as long term memory (LTM). Hurst (1951) first introduced the concept of LTM using the rescaled range (R/S) method in analyzing Nile river discharge. Since then, LTM has then been detected in precipitation, temperature and other climate and more general environmental data (e.g., Koscielny-Bunde *et al* 1998, Marani 2003, Bunde *et al* 2013, Yuan *et al* 2014). In mathematical terms, a time series with LTM has an autocorrelation function $C(n)$ following a power law $C(n) \sim n^\gamma$, with n as time scales, γ as the auto-correlation exponent, and its mean correlation time diverges for infinitely long series. This scaling behavior

can also be expressed as a fluctuation function $F(n) \sim n^\alpha$ with α as the DFA exponent, obtained from detrended fluctuation analysis (DFA), or the power law decay of the power spectrum function $S(f) \sim f^\beta$ with f as frequencies and β as the power spectrum exponent. β , α , and γ can be used to measure LTM and their relations are:

$$\beta = 2\alpha - 1; \alpha = 1 - \gamma/2. \quad (1)$$

Values of $0.5 < \alpha < 1$ indicate LTM; $\alpha = 0.5$ an uncorrelated process; $0 < \alpha < 0.5$ anti-correlation; $\alpha = 1$ is characteristic of $1/f$ noise; and $\alpha > 1$ marks a non-stationary and unbounded series.

LTM in global instrumental temperature data yields $\alpha \approx 0.5$ over inner continental areas in North America and central Asia, $\alpha \approx 0.65$ in coastal areas and $\alpha > 0.8$ over ocean for a time range from months to a few decades (Koscielny-Bunde *et al* 1998, Bunde and Havlin 2002, Fraedrich and Blender 2003,

Monetti *et al* 2003). Other work revealed distinct scaling regimes for precipitation over land, and generally smaller DFA exponents close to $\alpha = 0.5$ for the time range higher than days (Fraedrich and Larnder 1993, Marani 2003, Kantelhardt *et al* 2006). Due to the restricted length of instrumental data, the range of LTM in precipitation and temperature time series has been evaluated for periods up to a few years. However, the power spectra are reproduced in millennium long simulation of coupled atmosphere-ocean general circulation model, and the simulated LTM extends up to decadal and centennial time scales (Fraedrich and Blender 2003, Blender and Fraedrich 2006). Furthermore, by using Greenland ice cores data and simulations, the LTM for surface temperatures can even be extended to millennium scale (Blender *et al* 2006). Therefore, we assume no breaking down of the persistence law from inter-annual to centennial scales. As LTM is considered as a robust feature of internal atmosphere-ocean dynamics and independent on time-dependent external forcing (Hunt 1998, Blender and Fraedrich 2003, Blender *et al* 2006) and the variability is considered as a integral of a number of non-linear processes evolving on a wide range of time scales (Ashkenazy *et al* 2003), our analysis only focuses on the whole data period rather than individual periods.

Memory in proxy data has been identified almost half a century ago (Matalas 1962) by comparing first-order autocorrelation in the tree-ring series with first-order autocorrelation in theoretical precipitation/drought reconstructions. It was then further addressed in Stockton and Boggess (1980) and Meko (1981) introducing methods to correct the spectral biases. For example, lagging schemes were used by Stockton and Boggess (1980) to adjust for differences in autocorrelation between tree ring and river discharge data. Meko (1981) considered Box-Jenkins methods based on moving-mean autoregressive processes ARMA, to correct the behavior of autocorrelations at certain time-lags. The method was subsequently used in other tree-ring based climate reconstruction including Cook *et al* (1999) in their drought reconstruction. However, the memory was addressed more like short-term, as the autocorrelation was only considered at certain time-lags. Recently several papers have pointed out LTM in proxy data (e.g., Fraedrich *et al* 2009, Bunde *et al* 2013, Franke *et al* 2013, Barboza *et al* 2014, Kim *et al* 2014). Franke *et al* (2013) report that proxy data, including tree-ring width (TRW) and maximum late-wood density (MXD) chronologies, show different scaling characteristics including $\alpha = 0.75$ for precipitation sensitive TRW chronologies, and $\alpha = 0.85$ for temperature sensitive TRW chronologies. Bunde *et al* (2013) demonstrated the existence of LTM in TR based precipitation reconstructions. Their work revealed TR chronologies to contain larger LTM compared to observed temperature and precipitation. Since the power spectrum exponents β in Franke *et al* (2013) may contain relatively high uncertainties (Kim

et al 2014), and Bunde *et al* (2013) and other studies only analyzed few selected proxies or temperature/precipitation reconstructions, the character and range of LTM in TR proxies (TRW and MXD) still need to be assessed.

Here, we aim at (1) confirming the existence of climate-relevant or -irrelevant processes introducing LTM in TR data; (2) analyzing the scaling behavior in TR based climate reconstructions; (3) assessing the potential influences of modified LTM on climate reconstructions based on pseudo-proxy data. We therefore assess the LTM in a total of 231 world-wide distributed climate sensitive TR chronologies, as well as regional mean climate reconstructions from China by employing the DFA. China is an important region to reconstruct past climate, because it has a wide-range of climatic conditions and offers a variety of proxy data, primarily from tree-rings (e.g. Cook *et al* 2010).

To demonstrate the impact of LTM on reconstructed climate variability, we compare pseudo-instrumental data (without memory) and pseudo-reconstructions (with artificial LTM) derived from simulated (1155 years) precipitation in southeastern Asia (see section data for more details). For detailed temporal comparisons, we give an example using the data at grid-point [105E, 23.3N] for the full period (850–2005). This grid point is located at the border of Yangtze River region, one of the most important East-Asia Monsoon regions. For the spatial comparison of trends and anomalies, we show the evaluation from the pseudo-data in the period 1901–2005 years over southeastern Asia.

2. Data and Methodology

2.1. Data

Proxy and reconstructed data

We use 231 TR chronologies from across the globe, which include 133 TRW and 98 MXD site records starting before 1700 AD and ending in the late 20th century (mostly in 1998 AD). 15 (118) TRW datasets are interpreted as proxies for annual temperature (precipitation) variation; see table S1 for detailed information and figure S1 for their locations. All TRW chronologies are directly extracted from international tree ring data bank (ITRDB, Grissino-Mayer and Fritts 1997) and MXD mostly from Cook *et al* (2010). They are significantly correlated with gridded instrumental data (details see ‘table S1 and ‘table S2 in the appendix of Briffa *et al* 2002). Besides, we also use one TRW chronology representing precipitation in northeastern Tibet over the past 3,500 years (Yang *et al* 2014, here referred to as ‘Yang2014), and reconstructions of regional mean temperature/PDSI from various recent publications from China and East Asia (Cook *et al* 2010, Shi *et al* 2012, Ge *et al* 2013, and Yang *et al* 2002), here referred to as ‘Yang2012’, ‘Cook2010’, ‘Shi2012-EIV’, ‘Ge2013’, and ‘Yang2002’, respectively.

'Cook2010' is the regional mean of gridded annual PDSI reconstructions over East Asia. 'SHI2012-EIV' is the regional mean of gridded annual temperature reconstructions over China. 'SHI2012-EIV' is a decadally resolved temperature reconstruction over China derived from merging multiple proxies from nine different climate regions using an area weighting scheme. 'Ge2013' is also a decadally resolved regional mean temperature reconstruction over China derived from multi-proxies using a principal component regression method. 'Yang2012', 'Cook2010' and 'Shi2012-EIV' use only or primarily TR data; 'Yang2002' and 'Ge2013' use multi-proxy data.

Pseudo-instrumental and pseudo-reconstructed rainfall
The pseudo-instrumental precipitation data is directly extracted from model simulations at $1.875^\circ \times 1.875^\circ$ resolution in the area mostly covering Asia ($10\text{--}50^\circ\text{N}$, $65\text{--}135^\circ\text{E}$). The simulations are carried out using the Max Planck Institute Earth System Model for paleo application (MPI-ESM-P, Jungclaus *et al* 2014). The model consists of the spectral atmospheric model ECHAM6 (Stevens *et al* 2013) in T63L47 resolution, the ocean model MPIOM (Marsland *et al* 2003, Jungclaus 2013) in GR1.5L40 resolution and prescribed vegetation maps (Pongratz *et al* 2008). The model is run under PMIP3/CMIP5 protocols for the last millennium (850–1849, 'past1000') and the historical period (1850–2005, 'historical'). The runs 'past1000-r1' and 'historical-r1' over these periods were combined and are similar in length as most regional reconstructions from China.

The pseudo-reconstructed precipitation data are obtained by adding LTM to the pseudo-instrumental precipitation data. We use first Fourier-transform the time series, then change the scaling in the frequency domain $S(f) \sim f^\beta$, from the original value $\beta = 0$ to $\beta = 1$, and then inverse-transform back into the time domain. Note that this procedure of adding long-term persistence only slightly decreases the correlation between time series. We also tested a fractional integrated statistical model and generated time series with similar properties (details not shown here).

Even though, proxy time series normally contain additional noise giving them a lower signal-to-noise ratio compared to instrumental data, we avoid this additional complication here, but focus on the effects of the modified LTM on TR-based reconstructions. Both pseudo data sets are normalized by subtracting the mean and dividing the standard deviation over the whole period (850–2005). In this letter, extremes are defined here as annual values exceeding the upper and lower 5th percentiles of the time series.

2.2. Methodology

Considering the ability in dealing with non-stationary time series, and more accurate statistical outputs (Kim *et al* 2014), we apply the DFA method to diagnose

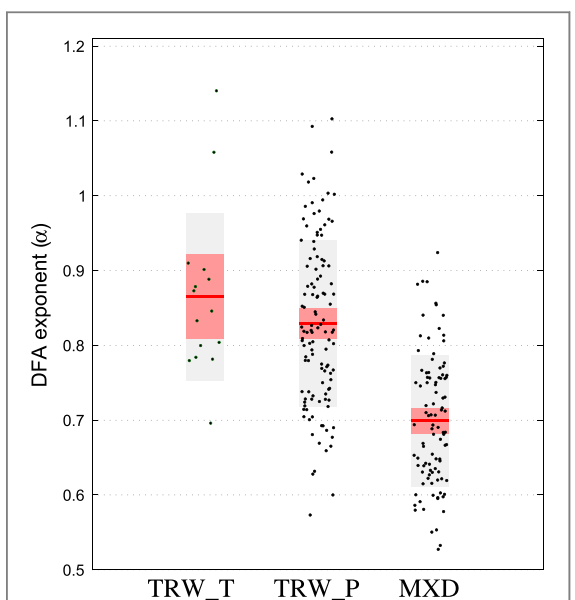


Figure 1. Fluctuation functions exponent H of tree-ring width sensitive to temperature (TRW_T) or rainfall (TRW_P), and of tree-ring maximum density (MXD) with a 1.96 standard error mean (95% confidence interval) in red and a 1.0 standard deviation in blue.

LTM in all the data we use in this letter (Peng *et al* 1994, Kantelhardt *et al* 2001).

Supposing we have N records x_i , we first subtract the mean and calculate the accumulated sum (profile)

$$X_n = \sum_{i=1}^n (x_i - \langle x_i \rangle). \quad (2)$$

Then, we divide the profile X_i into N_s non-overlapping segments Y_j of length s , as $N_s = [N/s]$, in each segment v , the 'local trend' $\widetilde{Y}_{j,v}$ is least squares fitting of variable order polynomials. Normally, quadratic polynomial fitting is enough for the accurate estimation of LTM in temperature/ rainfall records, therefore in this study we choose to use the quadratic polynomial fitting. We can determine the 'detrended walk' as the difference between the original profile $Y_{j,v}$ and the local trend $\widetilde{Y}_{j,v}$ and calculate the variance as

$$f_{\text{DFA}}^2(n, v) = \frac{1}{s} \sum_{j=(v-1)s+1}^{vs} (Y_{j,v} - \widetilde{Y}_{j,v})^2. \quad (3)$$

The detrended fluctuation function $F(n)$ is thus defined as

$$F_n = \sqrt{\frac{1}{N} \sum_{v=1}^{N_s} f_{\text{DFA}}^2(n, v)} \quad (4)$$

while N_s is the number of the windows, and $v = 1, 2, 3, \dots, N_s$. If $F_{\text{DFA}}(s)$ follows by a power law, $F_{\text{DFA}}(s) \sim s^\alpha$. As stated in the introduction, an exponent $\alpha > 0.5$ indicates a record x_i is long-term correlated. While $\alpha < 0.5$ indicates x_i is long-term anti-correlated. $\alpha = 0.5$ reveals white noise with no auto-correlation. Here, we use this exponent α to measure LTM, which is a generalization of the Hurst

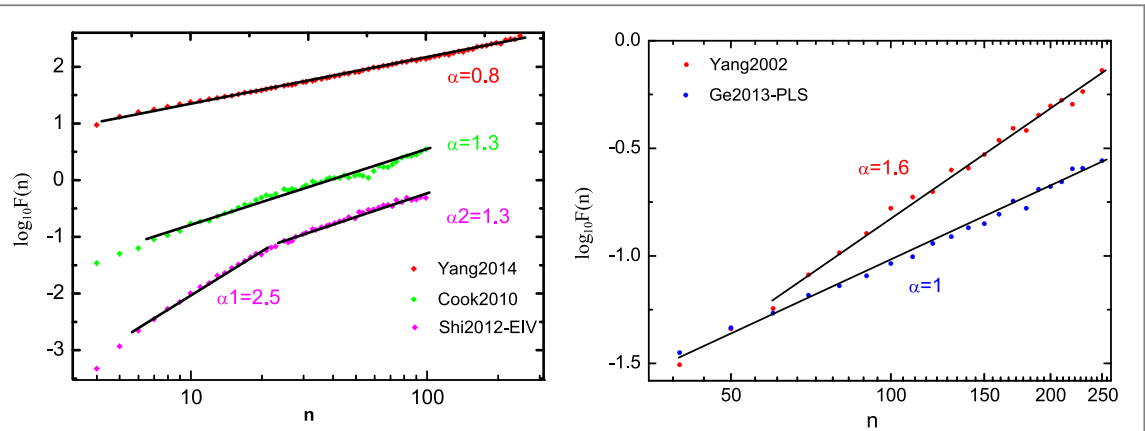


Figure 2. Fluctuation functions $F(n)$ for different field mean reconstructions over China. DFA exponents are indicated next to each line.

exponent and identifies long-time correlation, as well as the stationary/non-stationary nature of the data. DFA was applied to assess LTM in 15 temperature sensitive and 118 precipitation sensitive TRW records, as well as 98 MXD records (figure 1).

3. Results and Discussion

3.1. Long term persistence in single tree-ring chronologies

To illustrate how the DFA exponent is measured, we provide an example of precipitation sensitive TRW records, ‘Yang2014’, in northeastern Tibet (figure 1(a)). The fluctuation function shows a power law $F(n) \sim n^\alpha$ with $\alpha = 0.8$, ranging from 1 to more than 100 years. The DFA exponent of each TRW chronology is measured in this way indicating a mean of $\alpha = 0.86$ and $\alpha = 0.82$ from 1–50 years for the temperature and precipitation sensitive TRW time series, respectively. The scaling of some chronologies break at the time scale less than 50 years; this possibly depends on the length of tree core measurement series and the applied detrending methods (Briffa *et al* 1992, Cook *et al* 1995). The main climate drivers, temperature and precipitation, appear to have only limited influence on the TR proxy LTM as both land temperature and precipitation are characterized by weak-memory ($\alpha \approx 0.6$) and no-memory processes ($\alpha \approx 0.5$), respectively.

The same analysis using with 98 MXD times series reveals a mean $\alpha = 0.7$ for 1–50 years, consistent with the power spectrum exponent reported in Franke *et al* (2013). This indicates the existence of LTM in both TRW and MXD based reconstructions with TRW chronologies generally having higher DFA exponents compared to the MXD. One reason for lower DFA exponent values in the density data is that cell wall growth, as reflected by MXD, occurs over a shorter period in high and late summer, compared to TRW. TRW represent and integral of the cambial activity

throughout the growing season, though weighted towards early summer, and is additionally influenced by storage effects of carbohydrates during previous years. These biological carry-over effects increase the autocorrelation in TRW timeseries (Frank *et al* 2007).

3.2. Long term persistence in regional mean climate reconstructions over China

Except for climate reconstructions at single locations, intensified LTM is also detected in regional mean climate reconstructions integrating annually resolved TR data and decadally resolved multi-proxy data. The TRW based East-Asia mean annual PDSI reconstruction (‘Cook2010’ in figure 2) shows a nearly constant LTM $\alpha = 1.3$, on time scales between 1 year and 100 years. The reconstruction of annual mean temperatures over China (‘SHI2012-EIV’ in figure 2) shows two different scaling properties with $\alpha = 2.5$ from 1–20 years, and $\alpha = 1.3$ from 21–100 years. An explanation for the memory change is that high frequencies have been filtered out (using a 10-year low pass filter) in the initial data processing procedure (Shi *et al* 2012), which reddens the spectrum in the range 1–10 years. For the time range 20–100 years, the scaling exponent is consistent with the memory in ‘Cook2010’.

For Yang2002, we found a DFA exponent $\alpha = 1.6$, in line with the power spectrum exponent $\beta = 2$ reported in Zhang *et al* (2011). Finally, ‘Ge2013-PLS’ has a scaling with $\alpha = 1$ (figure 2).

These findings reveal that the regional PDSI and temperature reconstructions over China contain similar scaling exponents α ranging from 1.0 to 1.6 over time scales from 1 year to 100–200 years. Averaging single reconstructions over a large-scale area may increase α in the regional mean multi-proxy based temperature and PDSI reconstructions. Similarly, LTM of instrumental temperature over land is increased from $\alpha = 0.65$ at local and regional scales to $\alpha = 0.75$ at the global scale (Rypdal *et al* 2013). A

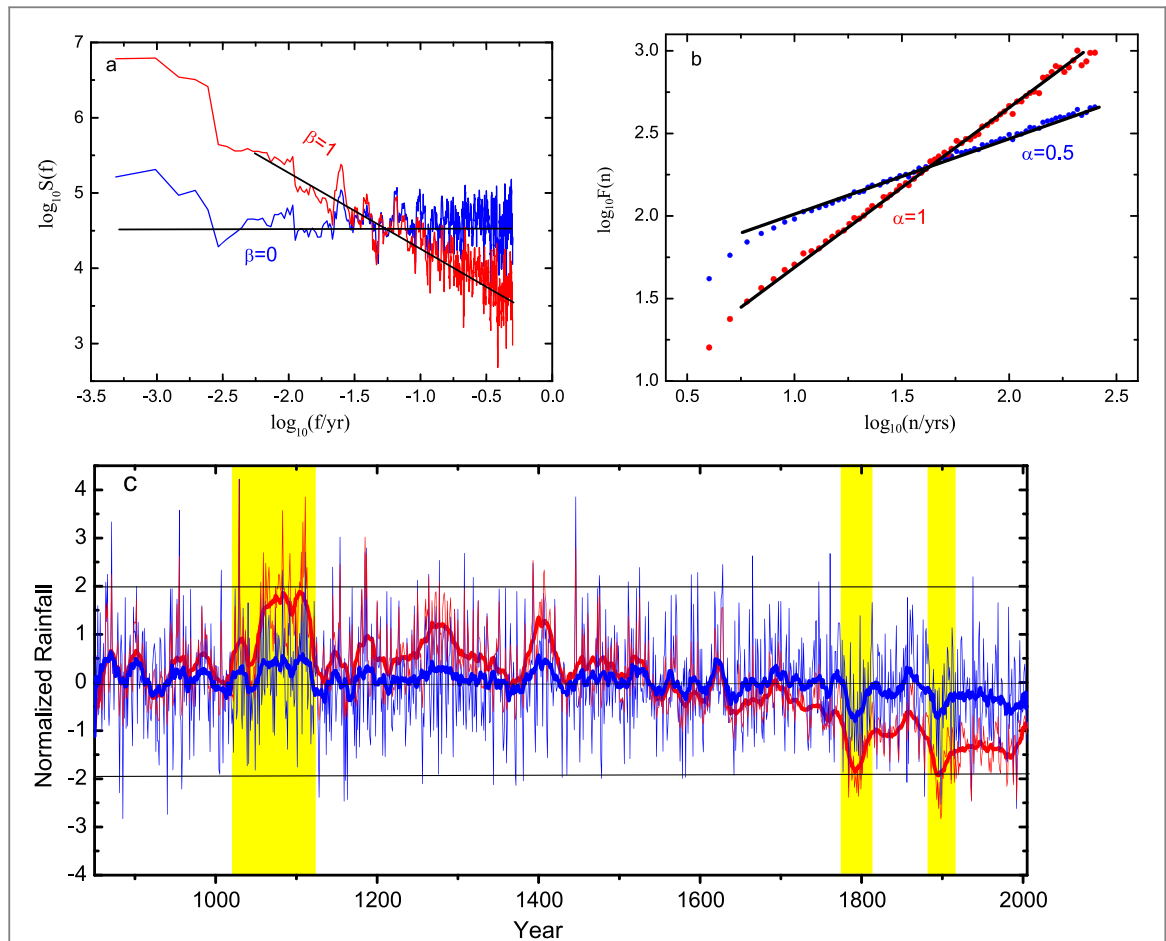


Figure 3. Power spectrum (a), fluctuation function (b) and annual (thin lines)/ 20 year-mean (thick lines) time series (c) of the grid point at [105E, 23.3N]. Blue: pseudo-instrumental data; Red: pseudo-reconstructions. Note the extreme clusters in yellow periods.

possible explanation is that for these larger scale climate products the spatial correlation among time series might increase the correlation with external forcing and decrease the high-frequency signal from the individual/local variability (Mann 2011).

3.3. Possible influences of intensified LTM on climate reconstruction

To demonstrate how the LTM can influence climate reconstructions, we perform an experiment to compare the no-memory pseudo-instrumental precipitation data with the with-memory pseudo-reconstructed precipitation in both time and spatial domain over southeastern Asia. The pseudo-proxy reconstructions are generated by artificially increasing low frequency variances of the pseudo-instrumental data at each grid point through the power spectrum transform as described in section 2.1.2.

Figure 3 shows an example of comparisons between pseudo-reconstructed precipitation time series and pseudo-instrumental, both extracted from the grid at [105E, 23.3N]. The pseudo-instrumental precipitation (thin blue lines in figure 3(c)) has a power-spectrum exponent $\beta = 0$ and DFA exponent $\alpha = 0.5$ (figure 3(a)). In the pseudo-reconstructed precipitation

both β and α equal 1. We smooth the data by using 20 yr moving average, as it is commonly used in reconstruction analysis to make the long-term fluctuations in the series stand out more clearly. Compared to the pseudo-instrumental precipitation, the pseudo-reconstructed time series contains several differing characteristics: the record at this specific grid point shows stronger low frequency variance and includes a generally wetter period 850–1500 followed by rather drier conditions 1500–2005. Wet/dry deviations appear more persistent with an increased chance that a wet year follows a wet year, and a dry year follows a dry year, a finding in agreement the assessment of precipitation reconstructions in Bunde *et al* (2013). Also, extreme events (the events passing the horizontal lines denoting the upper and lower 5th percentiles in figure 3(c)) more likely cluster in short periods as one main consequence of LTM (Bunde *et al* 2013), instead of being distributed randomly over time. Third, the pseudo-reconstructed precipitation contains a decreasing trend ($-2\%/\text{decade}$) according to linear regression analysis, compared to no significant trend in the pseudo-instrumental precipitation time series, as well as substantial trends in certain shorter periods, e.g. $8\%/\text{decade}$ compared to $-1\%/\text{decade}$ over the last 50 years.

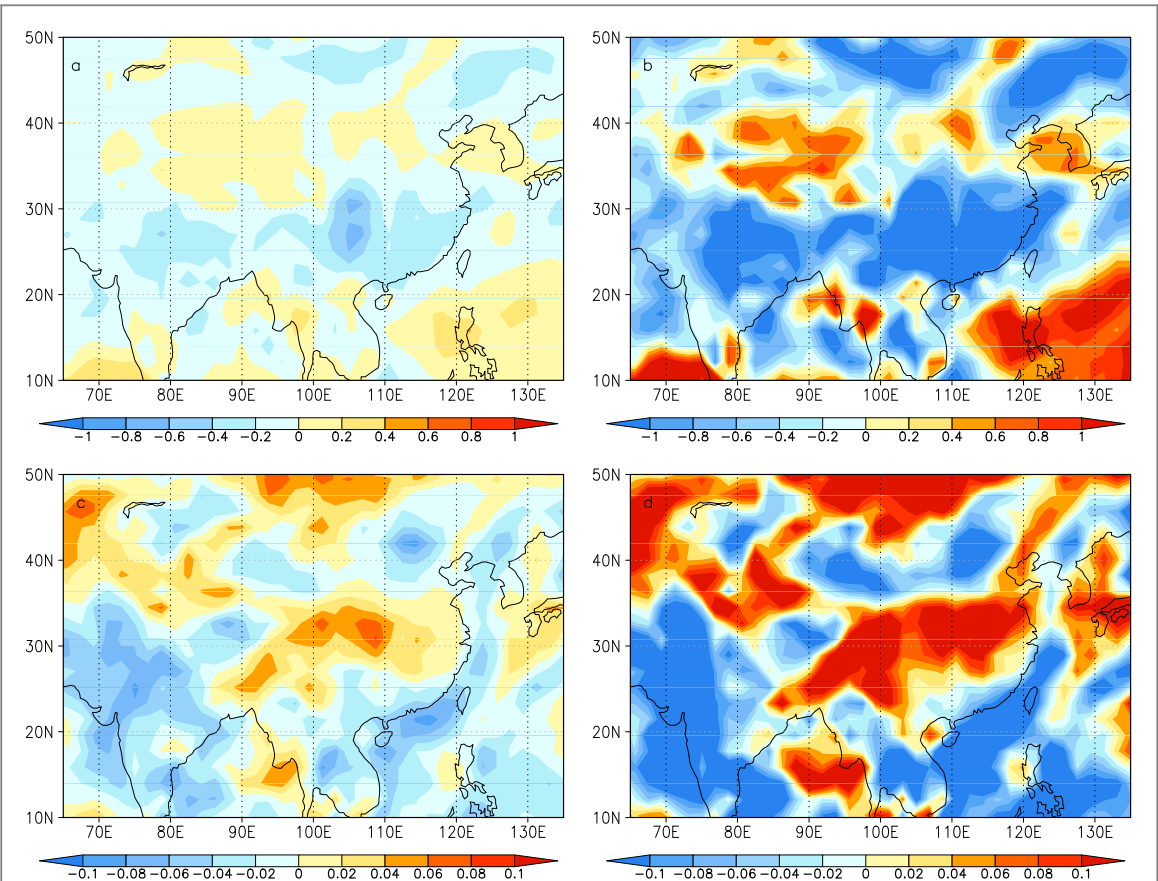


Figure 4. Normalized anomalies (a) and normalized trend per decade ((c), unit: 10^{-1} yrs) of pseudo-instrumental data for the period 1901–2005. Normalized anomalies (b) and normalized trend per decade ((d), unit: 10^{-1} yrs) of pseudo-reconstruction data for the same period.

To show the influences of modified LTM on reconstructed climate in space, we use the pseudo data to calculate anomalies and linear trends over the last 105 years in southeastern Asia. Figure 4 shows the values of the anomalies and trends are intensified in most regions. For example, while the anomalies of pseudo-instrumental precipitation from 1901 to 2005, relative to the 850–2005 climatology, range from -60% to -20% in southern China, the anomalies of pseudo-reconstructed precipitation reach $<-100\%$. The pseudo-reconstructed precipitation shows much stronger trends compared to the pseudo-instrumental precipitation over most of the region. For example, the pseudo-reconstructed precipitation has a positive trend ranging from $20\%–60\%/decade$ in the Yangtze river region, but the pseudo-reconstructed precipitation shows a positive trend exceeding $80\%/decade$ in this region. These findings show that climate reconstructions based on proxy data containing LTM can lead to exaggerated climate anomalies and trends in certain regions and specific time periods.

4. Conclusion

In this paper, we demonstrate that TR chronologies contain more LTM than climate observations. DFA is

applied to measure the strength of LTM in worldwide-distributed TR proxies and climate reconstructions (PDSI and temperature) from China. Our results reveal increased DFA exponent including mean value $\alpha = 0.8$ for TRW proxies and $\alpha = 0.7$ for maximum density data. For observational temperature and precipitation data, these values are smaller equaling $\alpha \approx 0.6$ and $\alpha \approx 0.5$, respectively. We consider that tree physiological processes influencing TRW are biasing the LTM in tree-ring proxies. LTM in single tree-ring (and other) proxies not only propagates into regional mean climate reconstructions, but is even accelerated in these larger scale products.

One main characteristic of data containing LTM is that the successive increments and layers are positively correlated, causing several effects which requiring attention. By comparing the pseudo-instrumental and pseudo-reconstructed precipitation we demonstrated that modified LTM may stimulate

- (i) additional trend during certain intervals, as well as over the whole reconstruction period, while the trends from external forcing tangling with the trends from intensified climate low-frequency variations; In this case, a new approach is suggested by Lennartz and Bunde (2011) and

Table A1. Information of the tree-ring chronologies.

Source/Publication	Site ID/chronid	Lat	Lon	Start year	End year	Data Type
ITRDB	ak020	60.6	-145.67	1365	1998	TRW_T
ITRDB	ak021	60	-141.68	1428	1998	TRW_T
ITRDB	arge013	-38.98	-71.05	1306	1998	TRW_T
ITRDB	arge091	-42.08	-71.83	320	1998	TRW_T
ITRDB	ca082	39.43	-122.68	1500	1998	TRW_T
ITRDB	ca529	36.45	-118.6	699	1998	TRW_T
ITRDB	ca630	38.7	-120	-420	1999	TRW_T
ITRDB	ca631	39.52	-120.55	930	1999	TRW_T
ITRDB	cana110	49.53	-123.03	1344	1998	TRW_T
ITRDB	mexi027	23.75	-105.75	1481	1998	TRW_T
ITRDB	nv513	38.9	-114.32	825	1998	TRW_T
ITRDB	wa064	48.17	-120.37	1487	1998	TRW_T
ITRDB	ar048	35.85	-90.95	1417	1998	TRW_P
ITRDB	ar049	34.95	-91.22	1133	1998	TRW_P
ITRDB	ar050	35.15	-91.3	1019	1998	TRW_P
ITRDB	ar052	35.55	-91.25	998	1998	TRW_P
ITRDB	ar053	33.77	-92.33	1262	1998	TRW_P
ITRDB	arge018	-39.22	-71.17	1392	1998	TRW_P
ITRDB	arge073	-41.03	-70.98	1497	1998	TRW_P
ITRDB	az084	36.17	-110.5	1470	1998	TRW_P
ITRDB	az086	36.83	-110.73	1365	1998	TRW_P
ITRDB	az102	36.68	-110.53	1490	1998	TRW_P
ITRDB	az106	35.82	-112.07	1448	1998	TRW_P
ITRDB	az129	36.63	-112.1	1482	1998	TRW_P
ITRDB	az144	36.83	-112.05	1481	1998	TRW_P
ITRDB	az520	32.38	-110.68	1460	1998	TRW_P
ITRDB	az547	35.17	-111.52	1420	1998	TRW_P
ITRDB	az557	32.45	-110.78	1321	1998	TRW_P
ITRDB	ca051	34.12	-116.82	-42	1998	TRW_P
ITRDB	ca073	41.77	-120.75	1310	1998	TRW_P
ITRDB	ca087	37.28	-119.08	1140	1998	TRW_P
ITRDB	ca528	36.77	-118.37	898	1998	TRW_P
ITRDB	ca529	36.45	-118.6	699	1998	TRW_P
ITRDB	ca531	36.77	-118.35	1027	1998	TRW_P
ITRDB	ca532	36.45	-118.62	1050	1998	TRW_P

Table A1. (Continued.)

Source/Publication	Site ID/chronid	Lat	Lon	Start year	End year	Data Type
ITRDB	ca533	37.5	-118.22	626	1998	TRW_P
ITRDB	ca535	37.43	-118.17	-6000	1998	TRW_P
ITRDB	ca612	34.65	-119.37	1470	1998	TRW_P
ITRDB	ca628	40.15	-120.6	1450	1998	TRW_P
ITRDB	ca629	41.45	-120.9	1152	1998	TRW_P
ITRDB	ca632	39.55	-120.2	1010	1999	TRW_P
ITRDB	ca633	37.75	-118.68	680	2000	TRW_P
ITRDB	canal35	51.17	-114.67	1315	1998	TRW_P
ITRDB	canal36	49.58	-114.22	1466	1998	TRW_P
ITRDB	canal37	49.58	-114.2	1467	1998	TRW_P
ITRDB	cana194	49.83	-97.2	1286	1999	TRW_P
ITRDB	chil002	-31.97	-71.03	1011	1998	TRW_P
ITRDB	co066	37.58	-108.55	1457	1998	TRW_P
ITRDB	co067	37.58	-108.55	1270	1998	TRW_P
ITRDB	co076	37.17	-108.52	1390	1998	TRW_P
ITRDB	co511	40.03	-105.58	1169	1998	TRW_P
ITRDB	co535	38.77	-104.97	1320	1998	TRW_P
ITRDB	co556	37.72	-105.47	1035	1998	TRW_P
ITRDB	co570	37.07	-103.27	1460	1998	TRW_P
ITRDB	co579	39.95	-106.52	1320	1999	TRW_P
ITRDB	co580	39	-108.15	1135	2000	TRW_P
ITRDB	fl001	30.47	-85.88	899	1998	TRW_P
ITRDB	ga002	31.62	-81.8	929	1998	TRW_P
ITRDB	ga003	32.35	-81.22	990	1998	TRW_P
ITRDB	ga004	32.05	-83.3	1202	1998	TRW_P
ITRDB	id006	42.52	-116.8	1492	1998	TRW_P
ITRDB	id009	44.6	-114.45	965	1998	TRW_P
ITRDB	id010	43.97	-114.97	955	1998	TRW_P
ITRDB	il016	37.27	-89.05	1468	1998	TRW_P
ITRDB	jord001	30.63	35.5	1469	1998	TRW_P
ITRDB	la001	32.25	-92.97	997	1998	TRW_P
ITRDB	mexi001	31.17	-115.5	1449	1998	TRW_P
ITRDB	mexi022	26.4	-106.08	1376	1998	TRW_P
ITRDB	mexi023	26.4	-106.08	1376	1998	TRW_P
ITRDB	mo037	36.57	-90.48	1185	1998	TRW_P
ITRDB	ms002	30.58	-88.58	1466	1998	TRW_P

Table A1. (Continued.)

Source/Publication	Site ID/chronid	Lat	Lon	Start year	End year	Data Type
ITRDB	nc008	34.32	-78.22	365	1998	TRW_P
ITRDB	nm025	35.6	-108.13	1381	1998	TRW_P
ITRDB	nm026	36.35	-106.52	1362	1998	TRW_P
ITRDB	nm030	35.4	-108.52	1411	1998	TRW_P
ITRDB	nm031	35.43	-108.53	1478	1998	TRW_P
ITRDB	nm035	34.22	-108.63	1490	1998	TRW_P
ITRDB	nm559	36.7	-105.43	1391	1998	TRW_P
ITRDB	nm560	36.73	-105.47	837	1998	TRW_P
ITRDB	nm564	34.22	-108.62	1410	1998	TRW_P
ITRDB	nm565	33.38	-108.23	1470	1998	TRW_P
ITRDB	nm572	34.97	-108.1	-136	1998	TRW_P
ITRDB	nv049	39.82	-114.62	1400	1998	TRW_P
ITRDB	nv052	39.1	-115.8	1470	1998	TRW_P
ITRDB	nv053	40.4	-114.22	1400	1998	TRW_P
ITRDB	nv055	38.68	-117.23	1490	1998	TRW_P
ITRDB	nv056	41.05	-114.58	1330	1998	TRW_P
ITRDB	nv058	39.18	-116.78	1439	1998	TRW_P
ITRDB	nv060	41.3	-118.43	1267	1998	TRW_P
ITRDB	nv061	41.9	-115.42	1334	1998	TRW_P
ITRDB	nv507	39.38	-114.92	1465	1998	TRW_P
ITRDB	nv510	36.27	-115.7	800	1998	TRW_P
ITRDB	nv514	40.55	-114.82	302	1998	TRW_P
ITRDB	nv515	39.08	-115.43	-2370	1998	TRW_P
ITRDB	nv516	38.93	-114.23	0	1998	TRW_P
ITRDB	nv518	41.3	-118.43	975	1998	TRW_P
ITRDB	or006	44.9	-118.93	1405	1998	TRW_P
ITRDB	or009	43.98	-118.8	1396	1998	TRW_P
ITRDB	or012	43.97	-121.07	1281	1998	TRW_P
ITRDB	or015	43.58	-120.45	1097	1998	TRW_P
ITRDB	or018	43.13	-119.87	1377	1998	TRW_P
ITRDB	or033	45.28	-118.57	1469	1998	TRW_P
ITRDB	or060	43.58	-120.45	870	1998	TRW_P
ITRDB	or061	43.97	-121.07	830	1998	TRW_P
ITRDB	or062	43.18	-120.9	530	1998	TRW_P
ITRDB	or063	42.67	-118.92	1017	1998	TRW_P
ITRDB	or081	42	-123.56	1420	2000	TRW_P

Table A1. (Continued.)

Source/Publication	Site ID/chronid	Lat	Lon	Start year	End year	Data Type
ITRDB	pola006	53.5	16	996	1998	TRW_P
ITRDB	sc004	33.18	-80.42	1001	1998	TRW_P
ITRDB	sd017	43.9	-103.6	1281	1998	TRW_P
ITRDB	spai011	40.18	-2.08	1485	1998	TRW_P
ITRDB	turk001	40	31.08	1306	1998	TRW_P
ITRDB	tx040	30.4	-94.07	1254	1998	TRW_P
ITRDB	tx042	29.25	-103.3	1473	1998	TRW_P
ITRDB	ut018	38.5	-109.25	1489	1998	TRW_P
ITRDB	ut022	37.02	-110.85	1469	1998	TRW_P
ITRDB	ut024	37.62	-109.73	1276	1998	TRW_P
ITRDB	ut508	39.42	-111.07	286	1998	TRW_P
ITRDB	va021	36.78	-76.88	932	1998	TRW_P
ITRDB	wy002	43.08	-110.07	1492	1998	TRW_P
ITRDB	wy006	43.7	-110.52	1400	1998	TRW_P
ITRDB	wy019	41.13	-106.05	1412	1998	TRW_P
ITRDB	wy026	41.87	-110.8	1480	1998	TRW_P
ITRDB	chin004x	34.48	110.08	1560	1998	MXD
ITRDB	co509x	37.18	-108.48	1373	1998	MXD
ITRDB	indi002x	35.08	74.3	1620	1998	MXD
ITRDB	indi006x	34.58	75.53	1654	1998	MXD
ITRDB	me010x	44.77	-70.77	1667	1998	MXD
ITRDB	nm529x	35.97	-108.8	1653	1998	MXD
Briffa <i>et al</i> (2002)	schweingruber_mxdabd_grid1	72.5	87.5	1400	1998	MXD
Briffa <i>et al</i> (2002)	schweingruber_mxdabd_grid10	67.5	17.5	1400	1998	MXD
Briffa <i>et al</i> (2002)	schweingruber_mxdabd_grid100	42.5	-107.5	1400	1998	MXD
Briffa <i>et al</i> (2002)	schweingruber_mxdabd_grid101	42.5	-72.5	1667	1998	MXD
Briffa <i>et al</i> (2002)	schweingruber_mxdabd_grid102	42.5	-2.5	1609	1998	MXD
Briffa <i>et al</i> (2002)	schweingruber_mxdabd_grid103	42.5	2.5	1612	1998	MXD
Briffa <i>et al</i> (2002)	schweingruber_mxdabd_grid104	42.5	7.5	1518	1998	MXD
Briffa <i>et al</i> (2002)	schweingruber_mxdabd_grid105	42.5	12.5	1540	1998	MXD
Briffa <i>et al</i> (2002)	schweingruber_mxdabd_grid106	42.5	17.5	1660	1998	MXD
Briffa <i>et al</i> (2002)	schweingruber_mxdabd_grid107	42.5	22.5	1583	1998	MXD
Briffa <i>et al</i> (2002)	schweingruber_mxdabd_grid108	37.5	-117.5	1513	1998	MXD
Briffa <i>et al</i> (2002)	schweingruber_mxdabd_grid109	37.5	-112.5	1453	1998	MXD
Briffa <i>et al</i> (2002)	schweingruber_mxdabd_grid111	67.5	22.5	1400	1998	MXD
Briffa <i>et al</i> (2002)	schweingruber_mxdabd_grid110	37.5	-107.5	1453	1998	MXD

Table A1. (Continued.)

Source/Publication	Site ID/chronid	Lat	Lon	Start year	End year	Data Type
Briffa <i>et al</i> (2002)	schweingruber_mxdabd_grid111	37.5	17.5	1441	1998	MXD
Briffa <i>et al</i> (2002)	schweingruber_mxdabd_grid112	37.5	22.5	1583	1998	MXD
Briffa <i>et al</i> (2002)	schweingruber_mxdabd_grid113	32.5	97.5	1406	1998	MXD
Briffa <i>et al</i> (2002)	schweingruber_mxdabd_grid115	27.5	97.5	1453	1998	MXD
Briffa <i>et al</i> (2002)	schweingruber_mxdabd_grid12	67.5	27.5	1400	1998	MXD
Briffa <i>et al</i> (2002)	schweingruber_mxdabd_grid13	67.5	32.5	1583	1998	MXD
Briffa <i>et al</i> (2002)	schweingruber_mxdabd_grid14	67.5	42.5	1583	1998	MXD
Briffa <i>et al</i> (2002)	schweingruber_mxdabd_grid15	67.5	52.5	1583	1998	MXD
Briffa <i>et al</i> (2002)	schweingruber_mxdabd_grid16	67.5	57.5	1400	1998	MXD
Briffa <i>et al</i> (2002)	schweingruber_mxdabd_grid17	67.5	62.5	1588	1998	MXD
Briffa <i>et al</i> (2002)	schweingruber_mxdabd_grid18	67.5	67.5	1400	1998	MXD
Briffa <i>et al</i> (2002)	schweingruber_mxdabd_grid19	67.5	72.5	1400	1998	MXD
Briffa <i>et al</i> (2002)	schweingruber_mxdabd_grid2	72.5	92.5	1400	1998	MXD
Briffa <i>et al</i> (2002)	schweingruber_mxdabd_grid20	67.5	77.5	1400	1998	MXD
Briffa <i>et al</i> (2002)	schweingruber_mxdabd_grid21	67.5	82.5	1400	1998	MXD
Briffa <i>et al</i> (2002)	schweingruber_mxdabd_grid22	67.5	87.5	1400	1998	MXD
Briffa <i>et al</i> (2002)	schweingruber_mxdabd_grid23	67.5	92.5	1583	1998	MXD
Briffa <i>et al</i> (2002)	schweingruber_mxdabd_grid24	67.5	97.5	1540	1998	MXD
Briffa <i>et al</i> (2002)	schweingruber_mxdabd_grid25	67.5	112.5	1450	1998	MXD
Briffa <i>et al</i> (2002)	schweingruber_mxdabd_grid26	67.5	117.5	1453	1998	MXD
Briffa <i>et al</i> (2002)	schweingruber_mxdabd_grid27	67.5	122.5	1564	1998	MXD
Briffa <i>et al</i> (2002)	schweingruber_mxdabd_grid28	67.5	127.5	1694	1998	MXD
Briffa <i>et al</i> (2002)	schweingruber_mxdabd_grid29	67.5	132.5	1669	1998	MXD
Briffa <i>et al</i> (2002)	schweingruber_mxdabd_grid3	72.5	102.5	1453	1998	MXD
Briffa <i>et al</i> (2002)	schweingruber_mxdabd_grid30	67.5	137.5	1481	1998	MXD
Briffa <i>et al</i> (2002)	schweingruber_mxdabd_grid31	67.5	147.5	1400	1998	MXD
Briffa <i>et al</i> (2002)	schweingruber_mxdabd_grid32	67.5	152.5	1556	1998	MXD
Briffa <i>et al</i> (2002)	schweingruber_mxdabd_grid33	62.5	-147.5	1554	1998	MXD
Briffa <i>et al</i> (2002)	schweingruber_mxdabd_grid34	62.5	-142.5	1583	1998	MXD
Briffa <i>et al</i> (2002)	schweingruber_mxdabd_grid36	62.5	-127.5	1697	1998	MXD
Briffa <i>et al</i> (2002)	schweingruber_mxdabd_grid38	62.5	-117.5	1612	1998	MXD
Briffa <i>et al</i> (2002)	schweingruber_mxdabd_grid39	62.5	-112.5	1610	1998	MXD
Briffa <i>et al</i> (2002)	schweingruber_mxdabd_grid4	72.5	112.5	1453	1998	MXD
Briffa <i>et al</i> (2002)	schweingruber_mxdabd_grid40	62.5	-102.5	1697	1998	MXD
Briffa <i>et al</i> (2002)	schweingruber_mxdabd_grid42	62.5	12.5	1400	1998	MXD
Briffa <i>et al</i> (2002)	schweingruber_mxdabd_grid44	62.5	22.5	1400	1998	MXD

Table A1. (Continued.)

Source/Publication	Site ID/chronid	Lat	Lon	Start year	End year	Data Type
Briffa <i>et al</i> (2002)	schweingruber_mxdabd_grid45	62.5	27.5	1400	1998	MXD
Briffa <i>et al</i> (2002)	schweingruber_mxdabd_grid46	62.5	32.5	1578	1998	MXD
Briffa <i>et al</i> (2002)	schweingruber_mxdabd_grid47	62.5	42.5	1578	1998	MXD
Briffa <i>et al</i> (2002)	schweingruber_mxdabd_grid48	62.5	52.5	1583	1998	MXD
Briffa <i>et al</i> (2002)	schweingruber_mxdabd_grid49	62.5	57.5	1583	1998	MXD
Briffa <i>et al</i> (2002)	schweingruber_mxdabd_grid5	72.5	117.5	1400	1998	MXD
Briffa <i>et al</i> (2002)	schweingruber_mxdabd_grid51	62.5	132.5	1683	1998	MXD
Briffa <i>et al</i> (2002)	schweingruber_mxdabd_grid52	62.5	137.5	1568	1998	MXD
Briffa <i>et al</i> (2002)	schweingruber_mxdabd_grid53	62.5	147.5	1400	1998	MXD
Briffa <i>et al</i> (2002)	schweingruber_mxdabd_grid54	62.5	152.5	1400	1998	MXD
Briffa <i>et al</i> (2002)	schweingruber_mxdabd_grid55	62.5	157.5	1400	1998	MXD
Briffa <i>et al</i> (2002)	schweingruber_mxdabd_grid56	57.5	-137.5	1697	1998	MXD
Briffa <i>et al</i> (2002)	schweingruber_mxdabd_grid57	57.5	-132.5	1686	1998	MXD
Briffa <i>et al</i> (2002)	schweingruber_mxdabd_grid58	57.5	-127.5	1697	1998	MXD
Briffa <i>et al</i> (2002)	schweingruber_mxdabd_grid59	57.5	-122.5	1697	1998	MXD
Briffa <i>et al</i> (2002)	schweingruber_mxdabd_grid6	72.5	127.5	1400	1998	MXD
Briffa <i>et al</i> (2002)	schweingruber_mxdabd_grid61	57.5	-92.5	1695	1998	MXD
Briffa <i>et al</i> (2002)	schweingruber_mxdabd_grid62	57.5	-77.5	1660	1998	MXD
Briffa <i>et al</i> (2002)	schweingruber_mxdabd_grid63	57.5	-72.5	1660	1998	MXD
Briffa <i>et al</i> (2002)	schweingruber_mxdabd_grid64	57.5	-67.5	1659	1998	MXD
Briffa <i>et al</i> (2002)	schweingruber_mxdabd_grid65	57.5	-7.5	1671	1998	MXD
Briffa <i>et al</i> (2002)	schweingruber_mxdabd_grid66	57.5	-2.5	1697	1998	MXD
Briffa <i>et al</i> (2002)	schweingruber_mxdabd_grid68	52.5	-127.5	1660	1998	MXD
Briffa <i>et al</i> (2002)	schweingruber_mxdabd_grid69	52.5	-122.5	1652	1998	MXD
Briffa <i>et al</i> (2002)	schweingruber_mxdabd_grid7	72.5	132.5	1400	1998	MXD
Briffa <i>et al</i> (2002)	schweingruber_mxdabd_grid70	52.5	-117.5	1400	1998	MXD
Briffa <i>et al</i> (2002)	schweingruber_mxdabd_grid8	72.5	137.5	1400	1998	MXD
Briffa <i>et al</i> (2002)	schweingruber_mxdabd_grid82	52.5	57.5	1671	1998	MXD
Briffa <i>et al</i> (2002)	schweingruber_mxdabd_grid84	52.5	87.5	1581	1998	MXD
Briffa <i>et al</i> (2002)	schweingruber_mxdabd_grid86	47.5	-127.5	1453	1998	MXD
Briffa <i>et al</i> (2002)	schweingruber_mxdabd_grid87	47.5	-122.5	1413	1998	MXD
Briffa <i>et al</i> (2002)	schweingruber_mxdabd_grid88	47.5	-117.5	1453	1998	MXD
Briffa <i>et al</i> (2002)	schweingruber_mxdabd_grid89	47.5	-112.5	1400	1998	MXD
Briffa <i>et al</i> (2002)	schweingruber_mxdabd_grid9	72.5	147.5	1434	1998	MXD
Briffa <i>et al</i> (2002)	schweingruber_mxdabd_grid90	47.5	-72.5	1697	1998	MXD
Briffa <i>et al</i> (2002)	schweingruber_mxdabd_grid91	47.5	-67.5	1697	1998	MXD

Table A1. (Continued.)

Source/Publication	Site ID/chronid	Lat	Lon	Start year	End year	Data Type
Briffa <i>et al</i> (2002)	schweingruber_mxdabd_grid92	47.5	7.5	1660	1998	MXD
Briffa <i>et al</i> (2002)	schweingruber_mxdabd_grid93	47.5	12.5	1660	1998	MXD
Briffa <i>et al</i> (2002)	schweingruber_mxdabd_grid94	47.5	17.5	1660	1998	MXD
Briffa <i>et al</i> (2002)	schweingruber_mxdabd_grid97	42.5	-122.5	1525	1998	MXD
Briffa <i>et al</i> (2002)	schweingruber_mxdabd_grid98	42.5	-117.5	1540	1998	MXD
Briffa <i>et al</i> (2002)	schweingruber_mxdabd_grid99	42.5	-112.5	1400	1998	MXD

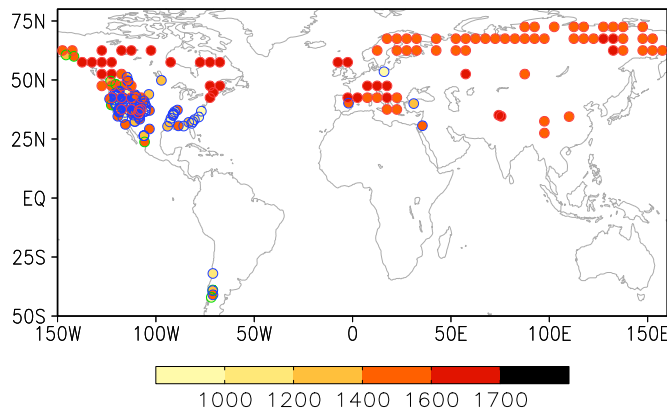


Figure A1. Location of the tree-ring chronologies. Colors of the circle frames indicate different data type: green for temperature, blue for rainfall and red for MXD. The filling color indicates the starting year of the chronology.

Tamazian *et al* (2015) to re-estimate the significance of trends in time series with LTM.

- (ii) increased low-frequency variance, and overestimated mean state of climate anomalies during certain periods;
- (iii) unrealistic deviations and extreme events in certain regions in spatially resolved reconstructions.

To modify the LTM in TR data, models based on fractionally integral techniques could be used as LTM is in fact a fractal phenomenon, such as the auto-regressive fractionally integrated moving-average model (ARFIMA) (Wei 1994) and the fractional integrated statistical model (Yuan *et al* 2014). Besides, since one TR chronology is typically developed by averaging data from multiple trees of limited lengths, first-order auto-regression or ARMA as a pre-whitening method (Meko 1981, Cook *et al* 1995) may be used during TR detrending to deduce long-term persistence. We here evaluate the influence of different detrending methods, which are commonly applied in dendrochronology (Cook *et al* 1995, Briffa *et al* 1992), and combine these approaches with an AR1 pre-whitening procedure to assess LTM in a temperature-sensitive TR chronologies from Siberia covering past 2,000 years. Results show that SLP300 combined with an AR1 pre-whitening procedure could change the LTM to approximate values found in instrumental temperatures (Figures not shown here). However, this analysis needs to be applied to more millennium long TR chronologies to further test whether the combination of AR1 and 300-year cubic smoothing splines (SLP300) can be generally used to adjust LTM in temperature-sensitive TR data.

The processes generating LTM in tree-ring data are still not fully understood. Likely, it is influenced by soil moisture supply, as precipitation-sensitive trees rather response to changes in root-zone soil moisture.

Soil moisture has an integrative behavior, and is possibly long-term persistent in dry areas (Blender and Fraedrich 2006, Wang *et al* 2010). Apart from that, it is also likely influenced by biological processes including carbohydrate storage and remobilization during cell wall construction and potential external disturbances and recovery of the forest structure (Frank *et al* 2007).

Acknowledgments

Support for PAGES Asia2k activities is provided by the US and Swiss National Science Foundations, US National Oceanographic and Atmospheric Administration and by the International Geosphere-Biosphere Programme. HZ acknowledges the German Science Foundation (DFG) project (Attribution of forced and internal Chinese climate variability in the common eras). NY and JL acknowledge also the LOEWE Large Scale Integrated Program (Excellency in research for the future of Hesse ‘FACE2FACE’). JPW gratefully acknowledges financial support by the Centre of Climate Dynamics (SKD), Bergen. UB was supported by the Czech project ‘Building up a multidisciplinary scientific team focused on drought’ (No. CZ.1.07/2.3.00/20.0248). We sincerely thank Frederick Reining for preparing the chronologies of the Siberia data and the reviewers for constructive comments and suggestions that improved the quality of the paper.

References

- Ashkenazy Y, Baker D R, Gildor H and Havlin S 2003 Nonlinearity and multifractality of climate change in the past 420,000 years *Geophys. Res. Lett.* **30** 2146
- Barboza L, Li B, Tingley M P and Viens F G 2014 Reconstructing past temperatures from natural proxies and estimated climate forcings using short- and long-memory models *Ann. Appl. Stat.* **8** 1966–2001
- Blender R and Fraedrich K 2003 Long time memory in global warming simulations *Geophys. Res. Lett.* **30**

- Blender R and Fraedrich K 2006 Long-term memory of the hydrological cycle and river runoffs in China in a high-resolution climate model *Int. J. Climatol.* **26** 1547–65
- Blender R, Fraedrich K and Hunt B 2006 Millennial climate variability: GCM-simulation and Greenland ice cores *Geophys. Res. Lett.* **33** L04710
- Briffa K R, Jones P D, Bartholin T S, Eckstein D, Schweingruber F H, Karlen W, Zetterberg P and Eronen M 1992 Fennoscandian summers from A.D.500: temperature changes on short and long timescales *Clim. Dyn.* **7** 111–9
- Briffa K R, Osborn T J, Schweingruber F H, Jones P D, Shiyatov S G and Vaganov E A 2002 Tree-ring width and density data around the Northern Hemisphere part 1, local and regional climate signals *Holocene* **12** 737–57
- Bunde A and Havlin S 2002 Power-law persistence in the atmosphere and in the oceans *Physica A* **314** 15
- Bunde A, Buentgen U, Ludescher J, Luterbacher J and von Storch H 2013 Is there memory in precipitation? *Nat. Clim. Change* **3** 174–5
- Cook E R, Anchukaitis K J, Buckley B M, D'Arrigo R D, Jacoby G C and Wright W E 2010 Asian monsoon failure and megadrought during the last millennium *Science* **328** 486–9
- Cook E R, Briffa K R, Meko D M, Graybill D A and Funkhouser G 1995 The 'segment length curse' in long tree-ring chronology development for palaeoclimatic studies *Holocene* **5** 229–37
- Cook E R, Meko D M, Stahle D W and Cleaveland M K 1999 Drought reconstructions for the continental United States *J. Clim.* **12** 1145–62
- Fraedrich K and Blender R 2003 Scaling of atmosphere and ocean temperature correlations in observations and climate models *Phys. Rev. Lett.* **90** 108501
- Fraedrich K, Blender R and Zhu X 2009 Continuum climate variability: Long-term memory, scaling, and 1/f-noise *Int. J. Mod. Phys. B* **23** 5403–16
- Fraedrich K and Larnder C 1993 Scaling regimes of composite rainfall time series *Tellus* **45A** 289–98
- Frank D, Bntgen U, Bhm R, Maugeri M and Esper J 2007 Warmer early instrumental measurements versus colder reconstructed temperatures: shooting at a moving target *Quat. Sci. Rev.* **26** 3298–310
- Franke J, Frank D, Raible C C, Esper J and Broennimann S 2013 Spectral biases in tree-ring climate proxies *Nat. Clim. Change* **3** 360–4
- Ge Q, Hao Z, Zheng J and Shao X 2013 Temperature changes over the past 2000 yr in China and comparison with the Northern Hemisphere *Clim. Past* **9** 1153–60
- Grissino-Mayer H D and Fritts H C 1997 The International Tree-Ring Data Bank: an enhanced global database serving the global scientific community *Holocene* **7** 235–8
- Hunt B G 1998 Natural climatic variability as an explanation for historical climatic fluctuations *Clim. Change* **38** 133–57
- Hurst H E 1951 Long-term storage capacity of reservoirs *Trans. Am. Soc. Civ. Eng.* **116** 770–808
- Jungclaus J H et al 2013 Characteristics of the ocean simulations in the Max Planck Institute Ocean Model (MPIOM) the ocean component of the MPI-Earth system model *J. Adv. Model. Earth Syst.* **5** 422–46
- Jungclaus J H, Lohmann K and Zanchettin D 2014 Enhanced XX century heat transfer to the Arctic simulated in the context of climate variations over the last millennium *Clim. Past Discuss* **10** 2895–924
- Kantelhardt J W, Koscielny-Bunde E, Rego H, Havlin S and Bunde A 2001 Detecting long-range correlations with detrended fluctuation analysis *Phys. A: Stat. Mech. Appl.* **295** 441–54
- Kantelhardt J W, Koscielny-Bunde E, Rybski D, Braun P, Bunde A and Havlin S 2006 Long-term persistence and multifractality of precipitation and river runoff records *J. Geophys. Res.* **111** D01106
- Kim B, Kim H and Min S 2014 Hurst's Memory for Chaotic, Tree Ring, and SOI Series *Appl. Math.* **5** 175–95
- Koscielny-Bunde E, Bunde A, Havlin S, Roman H E, Goldreich Y and Schellnhuber H-J 1998 Indication of a universal persistence law governing atmospheric variability *Phys. Rev. Lett.* **81** 729–32
- Lennartz S and Bunde A 2011 Distribution of natural trends in long-term correlated records: A scaling approach *Phys. Rev. E* **84** 021129
- Mann M E 2011 On long range dependence in global surface temperature series *Clim. Change* **107** 267–76
- Marani M 2003 On the correlation structure of continuous and discrete point rainfall *Water Resour. Res.* **39** 1128
- Marsland S J, Haak H, Jungclaus J H, Latif M and Roeske F 2003 The Max-Planck-Institute global ocean/sea-ice model with orthogonal curvilinear coordinates *Ocean Model.* **5** 91–127
- Matalas N C 1962 Statistical properties of tree ring data *Hydrolog. Sci. J.* **7** 39–47
- Meko D M 1981 Applications of Box-Jenkins methods of time series analysis to the reconstruction of drought from tree rings *PhD Dissertation* University of Arizona, Tucson
- Monetti R A, Havlin S and Bunde A 2003 Long-term persistence in the sea surface temperature fluctuation *Physica A* **320** 581–9
- Peng K, Buldyrev S V, Havlin S, Simonsf M, Stanley H E and Goldberger A L 1994 Mosaic organization of DNA nucleotides *Phys. Rev. E* **49** 1685–9
- Pongratz J C, Reick T, Raddatz and Claussen M 2008 A reconstruction of global agricultural areas and land cover for the last millennium, *Global Biogeochem Cycles* **22** GB3018
- Rypdal K, stvand L and Rypdal M 2013 Long-range memory in Earth's surface temperature on time scales from months to centuries *J. Geophys. Res.: Atmos.* **118** 7046–62
- Shi F, Yang B and von Gunten L 2012 Preliminary multiproxy surface air temperature field reconstruction for China over the past millennium *Sci. China Earth Sci.* **55** 2058–67
- Stevens B, Giorgetta M A, Esch M, Mauritsen T, Crueger T et al 2013 Atmospheric component of the MPI-M Earth System Model: ECHAM6 *J. Adv. Model. Earth Syst.* **5** 146–72
- Stockton C W and Boggess W R 1980 Augmentation of hydrologic records using tree rings *Improved Hydrologic Forecasting: Why and How* (Pacific Grove: ASCE) 239–65
- Tamazian A, Ludescher J and Bunde A 2015 Significance of trends in long-term correlated records *Phys. Rev. E* **91** 032806
- Wang G, Dolman A J, Blender R and Fraedrich K 2010 Fluctuation regimes of soil moisture in ERA-40 re-analysis data *Theor. Appl. Climatol.* **99** 1–8
- Wei WW 1994 *Time Series Analysis* (Addison-Wesley: Reading, MA)
- Yang B, Braeuning A, Johnson K R and Shi Y F 2002 General characteristics of temperature variation in China during the last two millennia *Geophys. Res. Lett.* **29** 1324–7
- Yang B, Qin C, Wang J, He M H, Melvin T M, Osborn T J and Briffa K R 2014 A 3,500-year tree-ring record of annual precipitation on the northeastern Tibetan Plateau *Proc. Natl Acad. Sci. USA.* **111** 2903–8
- Yuan N, Fu Z and Liu S 2014 Extracting climate memory using Fractional Integrated Statistical Model: a new perspective on climate prediction *Sci. Rep.* **4** 6577
- Zhang D, Blender R, Zhu X and Fraedrich K 2011 Temperature variability in China in an ensemble simulation for the last 1200 years *Theor. Appl. Climatol.* **103** 387–99